The Sixth KSME-JSME Thermal and Fluids Engineering Conference
Jeju, Korea, March 20-23, 2005
DD.02

Optimal Shape Design of Recuperators with Oblique Wavy Walls

Kenichi MORIMOTO*, Yuji SUZUKI and Nobuhide KASAGI

*Department of Mechanical Engineering, The University of Tokyo,
Hongo, Bunkyo-ku, Tokyo 113-8656, JAPAN
E-mail: morimoto@thtlab.t.u-tokyo.ac.jp

Keywords: Recuperator, Heat Transfer Enhancement, Wavy Wall

Abstract: A series of numerical simulation of the flow and heat transfer in modeled counter-flow heat exchangers with oblique wavy walls is made for optimal shape design of recuperators. The effects of oblique angles and height amplitudes of the wavy walls are systematically examined, and the heat transfer and pressure loss characteristics are investigated. Strong secondary flow is generated by counter-rotating streamwise vortices, which make the flow field highly asymmetric in the spanwise direction. With the oblique angle of 50-60 degree, significant heat transfer enhancement is achieved with relatively-small pressure loss penalty, and the *j*/*f* factor becomes significantly larger than that of straight square duct. When thermal coupling of hot and cold fluid passages is considered, the heat transfer is found to be strongly dependent on the arrangement of the passages. It is also found that the *j*/*f* factor is increased with the Reynolds number in the range of the present study.

1. Introduction

Small-scale distributed energy systems with micro gas turbines have been paid growing attention because of their high efficiency and low environmental impact. Recently, Uechi et al. (2004) showed that one of the most important technical issues for the system efficiency is to enhance the effectiveness of recuperator.

Among various types of compact heat exchangers proposed so far (e.g., Kays and London, 1984), primary surface recuperators have been considered promising and employed in recuperated turbine systems (McDonald, 2000). In heat-exchanger passages with modified surfaces, considerable heat transfer augmentation is attainable. However, the optimal shape of the flow passages, which maximizes heat transfer at the cost of minimal pressure loss, has not been obtained even in the laminar flow regime due to the complexity of heat and fluid flow phenomena.

In the present study, we propose a recuperator design with oblique wavy walls, and investigate the detailed mechanism of heat transfer enhancement. The emphasis is placed on the thermal coupling effect of counter-flowing fluids on the heat transfer performances.

2. Recuperator with oblique wavy walls

2.1 Recuperator configuration

Figure 1 shows the coordinate system and the passage geometry (over one pitch) with oblique wavy walls. Surface shapes of the top and bottom walls are defined as follows:

$$y_{w,\,top} = y_{w,\,bottom} = -A\cos 2\pi \big/ L_x \left(x - z\tan\gamma\right), \quad (1)$$

where A, L_x, and γ denote the amplitude, streamwise pitch, and oblique angle of the wavy walls, respectively. Two types of heat exchanger configurations with staggered arrangement of hot and cold fluids are assumed as shown in Fig. 2. Each passage is surrounded by oblique wavy walls (top and bottom walls) and flat side walls (left and right walls). The thermal resistance of dividing walls is neglected. The oblique angles of adjacent passages in Case 1 are the same in the spanwise (z-) direction, while those in Case 2 are identical in magnitude, but opposite in sign.

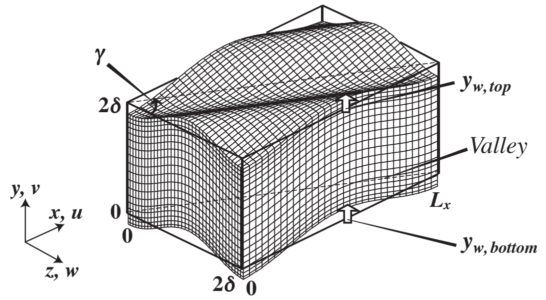

Figure 1. Surface geometry of the passage with oblique wavy walls and computational grids with a boundary fitted coordinate system.

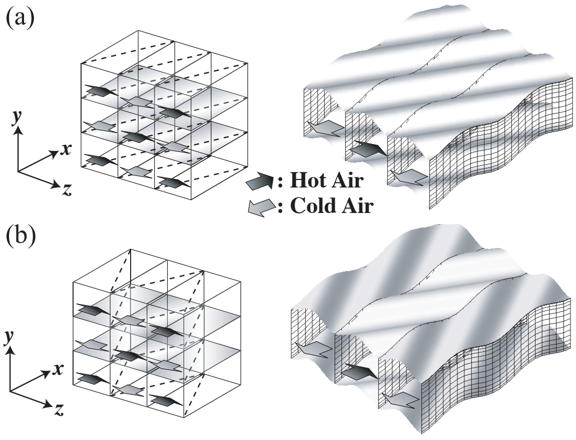

Figure 2. Configurations of modeled counter-flow recuperators: (a) Case 1, (b) Case 2.

In preliminary computations, we found that the most effective amplitude of wavy wall is 0.25δ. Thus, the amplitude is kept constant at 0.25δ throughout the present study.

2.2 Numerical method

The governing equations are the incompressible Navier-Stokes, continuity, and energy equations. The present numerical scheme is based on the finite difference method with general coordinate system. A second-order finite difference scheme is used for the spatial discretization. The flow is advanced in time by employing the SMAC method, assuring the continuity. Both counter-flowing fluids are air, and the bulk mean temperature is kept constant at each inlet. A periodic boundary condition is imposed in the streamwise (x-) direction. Isothermal heated walls are assumed when examining the heat transfer performance of an isolated passage. In order to evaluate the heat exchanger performances, the thermal coupling between the neighboring passages is considered by assuming the temperature and heat flux continuous over the dividing walls.

In the present study, the hydraulic diameter D_h of the duct is defined by its volume V and the wall surface area S_{total} as

$$D_h = \frac{4V}{S_{total}}, \tag{2}$$

in order to extract the effect of the geometrical change of the surfaces. Unless otherwise mentioned, the Reynolds number based on the bulk mean streamwise velocity and the hydraulic diameter is set constant at about 200. The Fanning friction factor f is defined by

$$f = \frac{(\Delta p/L_x)D_h}{2\rho U_b^2}, \tag{3}$$

where the pressure loss Δp represents the mean pressure difference between the inlet and outlet of the duct. The wall shear stress, the heat transfer coefficient, and the Nusselt number averaged over the wall surface are respectively defined as follows:

$$\langle \tau_w \rangle = \frac{1}{S_{total}} \frac{2D_h}{U_b} \int_S \frac{\partial u}{\partial n} dS, \tag{4}$$

$$h = \frac{q}{\Delta T_{lm}} = \frac{1}{S_{total}\Delta T_{lm}} \int_S -\lambda \left.\frac{\partial T}{\partial n}\right|_w dS, \tag{5}$$

$$\mathrm{Nu} = \frac{hD_h}{\lambda}, \tag{6}$$

where the log-mean temperature difference is defined by

$$\Delta T_{lm} = \frac{T_b(L_x) - T_b(0)}{\ln\{T_{w,m}(0) - T_b(0)\} - \ln\{T_{w,m}(L_x) - T_b(L_x)\}}. \tag{7}$$

The goodness factor of the present heat exchanger design is chosen as

$$\frac{j}{f} = \frac{\mathrm{Nu}\, Pr^{-1/3}}{f\,\mathrm{Re}}. \tag{8}$$

3. Heat transfer and pressure loss characteristics

3.1 Effect of oblique angles

Figure 3 shows the pressure loss and the friction drag normalized with those in straight square ducts versus the oblique angle γ. As γ decreases, the flow separation bubble described later is enlarged, and the pressure loss increases to $\gamma \sim 45^\circ$. The friction drag, on the other hand, takes its maximum value at $\gamma \sim 60^\circ$.

Figure 4 shows the averaged Nusselt number versus γ. The Nusselt number is significantly larger than that in straight square ducts, and takes its maximum value at $\gamma \sim 45^\circ$. It is also found that the thermal boundary condition has a large effect on the heat transfer performance. The Nusselt numbers for Case 1 are 22% lower than those for the isothermal wall condition, while the results for Case 2 are up to 5% lower. This drastic change can be explained by the flow and thermal fields in the duct described later.

Figure 5 shows the j/f factor versus γ. It can be seen that the j/f factor becomes larger than that of the corresponding straight duct by up to 25%. Although the Nusselt numbers are maximized at $\gamma \sim 45^\circ$, the pressure loss due to flow separation is also very large. Thus, the j/f factor has its peak at $\gamma \sim 60^\circ$, where the friction drag

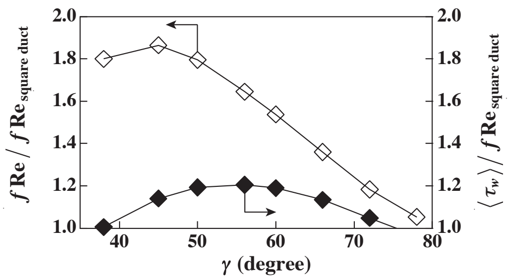

Figure 3. Pressure loss and friction drag versus oblique angle.

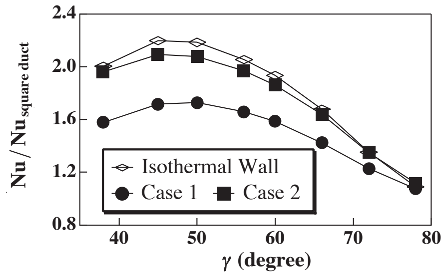

Figure 4. Averaged Nusselt number versus oblique angle.

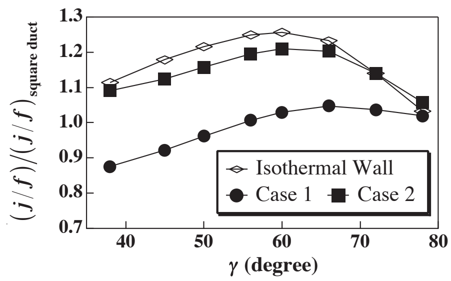

Figure 5. j/f factors versus oblique angle.

(a)

(b)

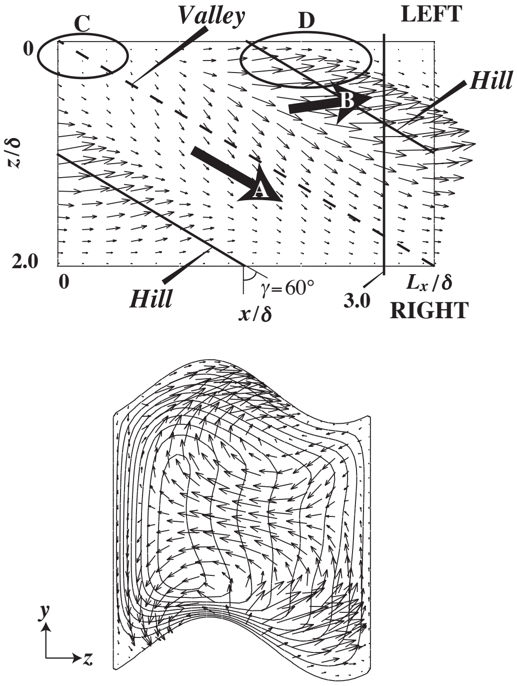

Figure 6. Flow field in wavy duct: (a) Wall shear stress vectors on the bottom wall projected onto the x-z plane, (b) Velocity vectors in the y-z plane at $x/\delta = 3.0$ and iso-contours of the streamwise velocity. The contour increment is $0.2U_b$.

(a)

(b)

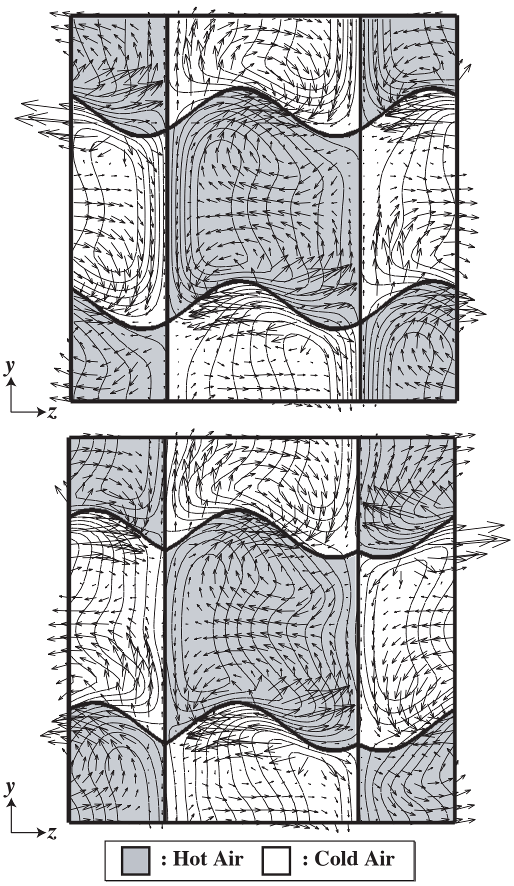

Figure 7. Velocity vectors and iso-contours of temperature under thermal coupling condition in the y-z plane at x/δ = 3.0 for $\gamma = 60°$. (a) Case 1, (b) Case 2.

(a)

(b)

(c)

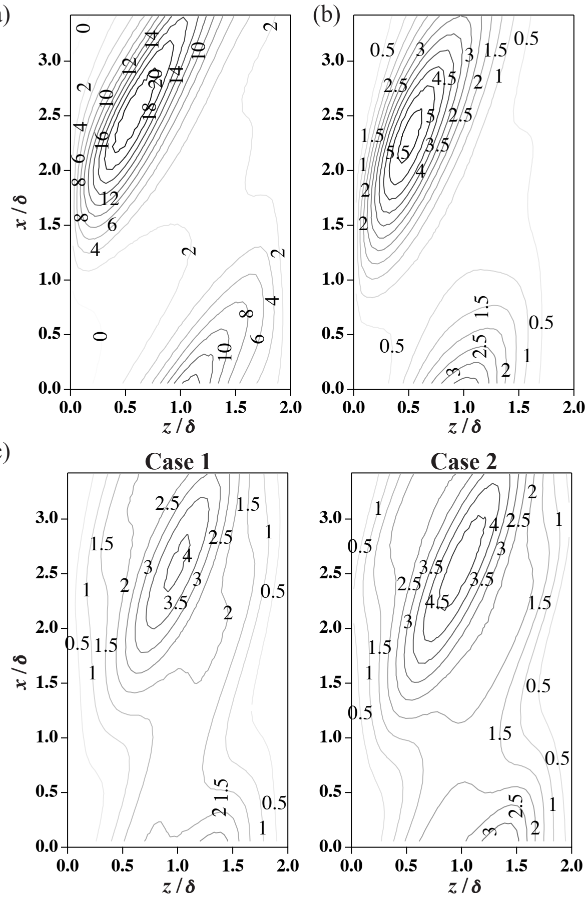

Figure 8. Distributions of the wall shear stress and the wall heat flux on the bottom wall: (a) Wall shear stress, (b) Heat flux on isothermal wall, (c) Heat flux under thermal coupling conditions (Cases 1 and 2).

becomes maximum as shown in Fig. 3. Therefore, it is conjectured that the heat transfer associated with wall shear flow is more effective than that with separation-reattachment flow in the present wavy ducts.

3.2 Mechanism of heat transfer enhancement

Hereafter, the oblique angle is kept constant at $\gamma = 60°$, and the detailed mechanism of heat transfer enhancement in the present recuperator is investigated.

Figure 6 shows wall shear stress vectors on the bottom wall, and velocity vectors in the y-z plane at $x/\delta = 3.0$ with iso-contours of the streamwise velocity. The oblique wavy wall induces a flow along the valley (A) and a flow over the hill toward the left wall (B). The flow along the wavy walls changes its direction upward by the interaction with the right wall. In combination with the vigorous flow over the hill toward the valley region, it forms a pair of counter-rotating vortices, which induce a flow toward the left wall at the center of the duct. The magnitude of this secondary flow is extremely large, and reaches up to 25% of the bulk mean streamwise velocity. Thus, the high-speed region is shifted to the left wall. The size of the flow separation bubble (C) is dependent on the magnitude of the flow over the hill near the left wall (D), and increased with decreasing γ.

Figure 7 shows the velocity vectors and iso-contours of temperature under the thermal coupling condition in the *y-z* plane. In Case 1, heat transfer is remarkably enhanced on the left wall of the central duct, since the side walls having higher heat transfer performances share the dividing wall. On the right wall, in contrast, heat transfer is markedly deteriorated, since the walls having lower performances share the wall. In Case 2, each of the side walls shares the walls with higher and lower performances, so that the total heat transfer is the same on the left and right walls. It is also observed that the dissimilarity between the velocity and temperature fields near the walls is more significant in Case 2 than in Case 1.

Figure 8 shows distributions of the wall shear stress and the wall heat flux on the bottom wall under different thermal boundary conditions. It can be seen that the wall shear stress and the heat flux on the isothermal wall exhibit a similar distribution and become large along the hill. The heat flux near the right wall remains small, because the streamwise velocity is small near the wall. On the other hand, the heat flux distributions in Cases 1 and 2 change their profiles due to the thermal coupling effect on both sides of the dividing wall, and the heat flux near the right wall is markedly increased. In Case 2, moreover, the heat transfer is augmented in broader regions over the wavy wall, and this results in heat transfer enhancement larger than in Case 1.

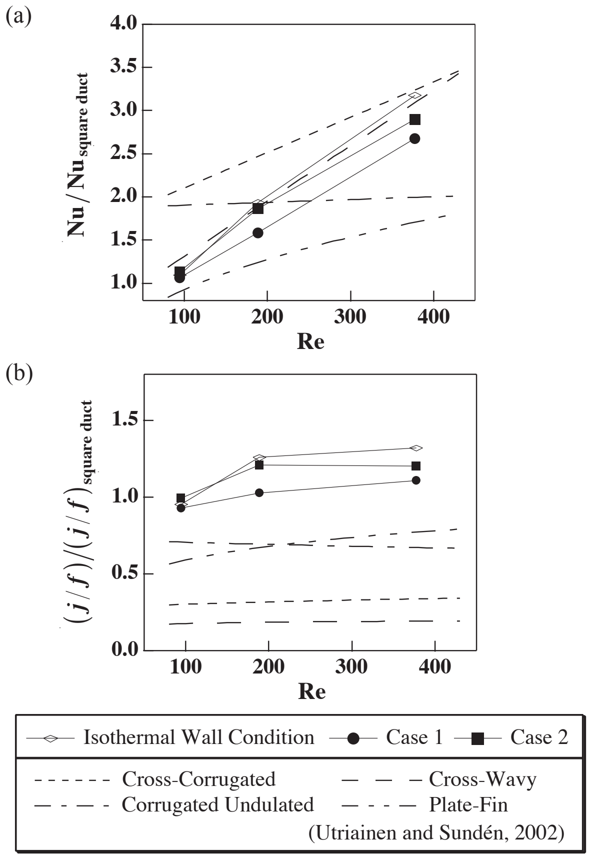

Figure 9. Effect of Reynolds number: (a) averaged Nusselt number, (b) *j/f* factor.

3.3 Reynolds number dependence

Figure 9 shows fRe, $\langle \tau_w \rangle$, Nu, and *j/f* for different Reynolds numbers. Performances of conventional compact heat exchangers (Utriainen and Sundén, 2002) are also plotted for comparison. It is found that, in the present recuperator, the Nusselt number profile is similar to that of the heat exchanger with cross wavy surfaces, while the *j/f* factor of the present recuperator is much larger than that of conventional ones because of the smaller pressure loss penalty. It is seen that the increase of *j/f* factor is gradually saturated with increasing the Reynolds number.

4. Conclusions

A series of numerical simulation of the flow and heat transfer in modeled counter-flow heat exchangers with oblique wavy walls is made for optimal shape design of recuperators. The effects of oblique angles and height amplitudes of the wavy walls are systematically evaluated, and the heat transfer and pressure loss characteristics are investigated. The flow field is drastically modified due to the counter-rotating streamwise vortices induced by the wavy walls. When the oblique angle is 50-60 degree, significant heat transfer enhancement is achieved at the cost of relatively-small pressure loss, and the *j/f* factor becomes significantly larger than that of straight duct or conventional recuperators. Since the flow field becomes highly asymmetric in the spanwise direction, the heat transfer is found to be strongly dependent on the arrangement of counter-flowing hot and cold fluid passages. Heat-exchanger performance is maximized when the side walls having larger and smaller heat transfer coefficients share the same dividing wall. It is also found that the *j/f* factor is increased with the Reynolds number in the range of the present study.

Acknowledgments

This work was supported through the CREST project, “Micro Gas Turbine and Solid Oxide Fuel Cell Hybrid Cycle for Distributed Energy System,” by JST. The first author (KM) was also supported by the Grant-in-Aid for JSPS Fellows (No. 15-11654) of MEXT of Japan.

References

Kays, W. M., and London, A. L., 1984, *Compact Heat Exchangers*, 3rd ed., McGraw-Hill, New York.

McDonald, C. F., 2000, Low-Cost Compact Primary Surface Recuperator Concept for Microturbines, Appl. Therm. Eng., **20**, pp. 471-497.

Uechi, H., Kimijima, S., and Kasagi, N., 2004, Cycle Analysis of Gas Turbine-Fuel Cell Cycle Hybrid Micro Generation System, ASME J. Eng. Gas Turbines Power, **126**, pp. 755-762.

Utriainen, E., and Sundén, B., 2002, Evaluation of the Cross Corrugated and Some Other Candidate Heat Transfer Surface for Microturbine Recuperators, ASME J. Eng. Gas Turbines Power, **124**, pp. 550-560.